Larval Anatomy of Andean Toads of the Rhinella spinulosa Group (Anura: Bufonidae)

Herpetological Monographs

Larval Anatomy of Andean Toads of the Rhinella spinulosa Group (Anura: Bufonidae)

--Manuscript Draft--

Manuscript Number:	HERPMONOGRAPHS-D-20-00001R2
Full Title:	Larval Anatomy of Andean Toads of the Rhinella spinulosa Group (Anura: Bufonidae)
Article Type:	Research Article
Keywords:	Buccal cavity; Chondrocranium; Musculature; Tadpoles
Abstract:	The Rhinella spinulosa group is a clade of toads that inhabit the Andes mountains from northern Ecuador to Patagonia. Its taxonomy was recently revised, and in its new arrangement comprises nine species, including Rhinella gallardoi traditionally placed in a different intrageneric group. In this work we studied the larval external and internal morphology in this group, by describing for the first time tadpoles of R. achalensis , R. gallardoi , and R. vellardi , and then summarizing morphological data for R. altiperuviana , R. limensis , R. papillosa , R. spinulosa , and R. trifolium . Although we found no diagnostic larval features for the whole clade, two distinct morphs were identified. Most tadpoles were highly pigmented and slender, and their oral discs showed a long gap in the second labial tooth row; conversely, tadpoles of R. limensis and R. vellardi shared a globose body and a very short gap. Buccal and musculoskeletal features were highly conserved within the group and regarding other Rhinella , and included four lingual papillae, non-keratinized spurs, tripartite suprarostral cartilages, quadratoorbital commissure, and in musculature, m. subarcualis rectus II–IV invading the branchial septum III and laryngeal muscles reduced or absent.
Response to Reviewers:	

Larval Anatomy of Andean Toads of the *Rhinella spinulosa* Group (Anura: Bufonidae)

FLORENCIA VERA CANDIOTI[1,7], JIMENA GROSSO[1], MARTÍN O. PEREYRA[2,3], M. BELÉN HAAD[1], JULIÁN LESCANO[4], KAREN SIU-TING[5,6], CÉSAR AGUILAR[6], AND DIEGO BALDO[3]

[1] Unidad Ejecutora Lillo (CONICET - FML), 4000 San Miguel de Tucumán, Argentina

[2] Museo Argentino de Ciencias Naturales "Bernardino Rivadavia" (CONICET), C1405 DJR Capital Federal, Argentina

[3] Laboratorio de Genética Evolutiva "Claudio Juan Bidau", Instituto de Biología Subtropical (CONICET - UNaM), Facultad de Ciencias Exactas, Universidad Nacional de Misiones, 3300 Posadas, Argentina

[4] Centro de Zoología Aplicada (CONICET), Facultad de Ciencias Exactas, Físicas y Naturales, Universidad Nacional de Córdoba, 5000 Córdoba, Argentina

[5] Institute for Global Food Security, School of Biological Sciences, Queen's University Belfast, BT9 5DL Belfast, United Kingdom

[6] Departamento de Herpetología, Museo de Historia Natural, Universidad Nacional Mayor de San Marcos, 15072 Lima, Perú

[7] CORRESPONDENCE: e-mail, florivc@gmail.com

ABSTRACT: The *Rhinella spinulosa* group is a clade of toads that inhabit the Andes mountains from northern Ecuador to Patagonia. Its taxonomy was recently revised, and in its new arrangement comprises nine species, including *Rhinella gallardoi* traditionally placed in a different intrageneric group. In this work we studied the larval external and internal morphology in this group, by describing for the first time tadpoles of *R. achalensis*, *R. gallardoi*, and *R. vellardi*, and then summarizing morphological data for *R. altiperuviana*, *R. limensis*, *R. papillosa*, *R. spinulosa*, and *R. trifolium*. Although we found no diagnostic larval features for the whole clade, two distinct morphs were identified. Most tadpoles were highly pigmented and slender, and their oral discs showed a long gap in the second labial tooth row; conversely, tadpoles of *R. limensis* and *R. vellardi* shared a globose body and a very short gap. Buccal and musculoskeletal features were highly conserved within the group and regarding other *Rhinella*, and included four lingual papillae, non-keratinized spurs, tripartite suprarostral cartilages, quadratoorbital commissure, and in musculature, m. subarcualis rectus II–IV invading the branchial septum III and laryngeal muscles reduced or absent.

Key words: Buccal cavity; Chondrocranium; Musculature; Tadpoles

THE NEOTROPICAL genus of toads *Rhinella* currently comprises 92 species assigned to seven phenetic groups, the *R. acrolopha* /*R. festae*, *R. crucifer*, *R. granulosa*, *R. margaritifera*, *R. marina*, *R. spinulosa*, and *R. veraguensis* groups (Duellman and Schulte 1992; Pramuk 2006; Grant and Bolivar-G 2014; Moravec et al. 2014), some of which are still poorly diagnosed (Pereyra et al. 2015). The *Rhinella spinulosa* species group includes medium to large-sized toads, very resistant to dryness and altitude (Cei 1960), distributed on both sides of the Andes mountain range and in sub-Andean mountain systems, from northern Ecuador to the Patagonian forests of southern Argentina and Chile, and from sea level to 5000 m asl. These toads inhabit and

reproduce mainly in rivers and streams, oviposit strings of eggs (uniserial, biserial, or multiserial) in a gelatinous tube (see Pereyra et al. 2015), and have exotrophic larvae, which usually develop in lotic environments.

The taxonomy of the species of the *Rhinella spinulosa* group was highly controversial and different authors disagreed on the specific or subspecific status of some taxa (e.g., Vellard 1959; Cei 1971; Duellman and Schulte 1992; Córdova 1999; Haas 2002). Traditionally, this group was composed of nine species: *R. achalensis*, *R. amabilis*, *R. arequipensis*, *R. arunco*, *R. atacamensis*, *R. limensis*, *R. rubropunctata*, *R. spinulosa* (including several subspecies), and *R. vellardi* (Frost 2019). However, the validity of the group was argued following recent molecular phylogenies that place *R. arunco* and *R. atacamensis* outside of the monophyletic group joining the remaining species (e.g., van Bocxlaer et al. 2010; Pyron 2014; Jetz and Pyron 2018). In addition, *R. gallardoi* is morphologically similar to *R. spinulosa* but it was not assigned to the *R. spinulosa* group due the presence of wide frontoparietals typical of species of the *R. veraguensis* and *R. margaritifera* groups (Carrizo 1992). Recent molecular evidence (M.O. Pereyra, personal observation) supports a restricted monophyletic *R. spinulosa* group composed of nine species: 1) four original members, i.e., *R. achalensis*, *R. amabilis*, *R. limensis*, and *R. vellardi*; 2) *R. altiperuviana*, *R. papillosa*, and *R. trifolium* erected at species level; 3) *R. spinulosa* sensu stricto, including *R. arequipensis*; and 4) *R. gallardoi* now recovered within this group. Features of larval external morphology are known for most of these species (Fernández 1927; Cei 1980; Sinsch 1986; Haas 2002; Angulo and Aguilar 2003; Aguilar and Gamarra 2004; Aguilar et al. 2007a), whereas data on internal morphology were described for only two of them (Aguilar and Pacheco 2005; Vera Candioti 2007).

In this work we revised larval external and internal morphology of the *Rhinella spinulosa* group. We first included formal description of the unknown tadpoles of three species *R.*

achalensis, *R. gallardoi*, and *R. vellardi*, and then we compared and summarized morphological descriptions of five more, clarifying taxonomic and nomenclatorial issues in previous literature. We finally explored buccal and musculoskeletal features to discuss the scarce information about larval internal morphology of the *R. spinulosa* group, and compared against what is known in other species groups in *Rhinella*.

MATERIALS AND METHODS

We studied 14 lots of tadpoles belonging to eight nominal species (*Rhinella achalensis*, *R. altiperuviana*, *R. gallardoi*, *R. limensis*, *R. papillosa*, *R. spinulosa*, *R. trifolium*, and *R. vellardi*), and two populations from Argentina (Catamarca and Mendoza Provinces, now on *Rhinella* aff. *spinulosa* CAT and MZA respectively). We collected tadpoles in several localities of Argentina and Perú; their taxonomic identity was confirmed by the combination of specimens reared to metamorphosis, DNA barcoding (16S gen), and unequivocal geographic distributions. We euthanized larvae with the anaesthetic MS222, and preserved them in 4% formalin. Voucher material is housed at herpetological collections of Laboratorio de Genética Evolutiva (IBS, CONICET – UNaM; LGE), Museo Argentino de Ciencias Naturales (CONICET; MACN), and Museo de Historia Natural (UNMSM; MUSM). Details of each lot are consigned in the Appendix.

We used two to twenty specimens per species (stages 29–38; Gosner 1960) for description and measurements of external morphology with a Leica M205 stereomicroscope. We colored tadpoles with a 1% solution of methylene blue to enhance visualization of some soft tissues (e.g., oral structures, spiracle). Measurements follow those proposed by Lavilla (1983) and Altig and McDiarmid (1999): total length, body length, maximum body width, body width at nares, body width at eyes, maximum body height, tail length, tail muscle height, maximum tail height, naris

length, extranarial distance, internarial distance, eye diameter, extraorbital distance, interorbital distance, rostro-spiracular distance, fronto-narial distance, eye-nares distance, oral disc width, dorsal gap width, and ventral gap width.

We dissected one to six specimens per species (stages 31–38) for internal anatomy description. We exposed buccopharyngeal cavity through a longitudinal cut below the tadpole eye, and used methylene blue to stain buccal papillae (Wassersug 1976a). For description of the musculoskeletal system, we used specimens cleared and stained according to Wassersug's protocol (1976b). To preserve the muscles from KOH digestion, we interrupted the procedure before that step and used Lugol's stain (Bock and Shear 1972) to visualize orange muscles against blue cartilages. External morphology terminology follows that of Altig and McDiarmid (1999), Altig (2007), and Lannoo (1987) for lateral lines. Terminology for buccal cavity and musculoskeletal features follow those of Wassersug (1976a) and Haas (2003), respectively. Unless they are not available, we used English names for skeletal structures instead of Latin terms.

RESULTS

External Morphology

Tadpoles of *Rhinella achalensis*, *R. gallardoi*, and *R. vellardi* were fully described in the paragraphs below. Morphological variations in the already described tadpoles of *R. limensis* (Angulo and Aguilar 2003; Aguilar et al. 2007a; as *Bufo limensis*), *R. papillosa* (Cei 1980; as *B. spinulosus papillosus*), *R. spinulosa* (Aguilar and Gamarra 2004; as *B. arequipensis*), *R. trifolium* (Sinsch 1986; Haas 2002; Aguilar and Gamarra 2004; Aguilar et al. 2007a; as *R. spinulosus* or *R. s. flavolineatus*, *R. s. trifolium*, and *R. s. spinulosus*), *R. altiperuviana* and *R.* aff. *spinulosa* CAT

(Fernández 1927; as *B. spinulosus*), and *R.* aff. *spinulosa* MZA (Cei 1980; as *B. s. spinulosus*) are summarized next.

Rhinella achalensis.—(Figs. 1A, 2A; *n* = 8, stages 32–35) Body depressed and oval from dorsal view; maximum width at the otic region. Snout slightly truncate in dorsal view and sloped in lateral view. Ventral body contour with a shallow depression in the gular region and convex in the abdomen. Nostrils large (6.5% of maximum width of body), dorsal, rounded, with an elevated marginal rim and a triangular medial projection; nostrils closer to the tip of the snout than to the eyes. Eyes large (20% of maximum width of body) and dorsolateral. Pineal end organ not visible. Spiracle sinistral and placed at the posterior half of the body, short, conical, posterodorsally oriented; external wall slightly folded dorsal and ventrally, giving an appearance of spiracle free from the body wall, but inner wall absent; small oval opening with its major axis oriented dorsoventrally. Gut switchback point medial or slightly displaced to the left of the abdominal cavity. Vent tube short and cylindrical, directed medially and opened dextral, margin fused to the ventral fin. Tail 1.6 longer than the body, with maximum height near to the distal third; dorsal fin originating at the body-tail junction, with the first portion low and almost parallel to the longitudinal body axis and then curved and taller; ventral fin as tall as the dorsal fin and uniformly high; tail tip widely rounded. Tail as high as the body (ratio between body maximum height and maximum tail height is about 1). Caudal musculature thick, tapering distally without reaching the tail tip. Lateral lines not visible. Oral disc (Fig. 2A) large (43% of maximum width of body), ventral, and emarginated; marginal papillae in a single row, with wide dorsal and ventral gaps (84% and 58% of the oral disc width, respectively); submarginal papillae scarce (1–3) and mainly on the upper commissure; jaw sheaths darkly colored, serrated, and with similar width, the upper sheath gently curved with distal ends oriented posterolaterally, and the lower

sheath smaller and V-shaped. Labial tooth row formula 2(2)/3(1); gap in A2 row about 20 teeth wide, and gap in P1 very short, about 4–5 teeth wide; labial teeth are curved, with a wide sheath, scarcely marked neck, and head with 12–14 marginal cusps (Fig. 4A). Coloration: in preserved specimens, dorsum and lateral sides of the body uniformly brown, venter opaque grey and brown with melanophores concentrated on the gular region where the adhesive gland regressed. A dark, straight dorsal line (which in early embryos points out the distribution of cells of the hatching gland) still visible at the analyzed stages, from the nares level to the base of the tail muscles. Tail musculature lighter, lacking melanophores at the muscle-fin junctions; dorsal fin and the posterior third of the ventral with melanophores uniformly distributed, and remaining portions of the ventral fin with disperse melanophores.

Rhinella gallardoi.—(Figs. 1B, 2B; *n* = 10, stages 29–31) Body slightly depressed and oval from dorsal view; maximum width at the otic region. Snout widely truncate in dorsal view and rounded in lateral view. Ventral body contour slightly convex in the abdomen. Nostrils large (7% of maximum width of body), dorsal, rounded, with a slightly elevated rim and a barely outlined medial projection; nostrils closer to the tip of the snout than to the eyes. Eyes large (17% of maximum width of body) and dorsolateral. Pineal end organ not visible. Spiracle sinistral and placed at the middle third of the body, short, conical, posterodorsally oriented; inner wall absent and small oval opening with its major axis oriented dorsoventrally. Gut switchback point medial or slightly displaced to the left of the abdominal cavity. Vent tube short and cylindrical, directed medially and opened dextral, margin fused to the ventral fin. Tail is 1.4 larger than the body, with maximum height near to the distal third; dorsal fin originating at the body-tail junction, with the first portion low and almost parallel to the longitudinal body axis and then curved and taller; ventral fin lower than the dorsal fin and uniformly high; tail tip narrowly rounded. Tail slightly

lower than the body (ratio between body maximum height and maximum tail height is about 1.1). Caudal musculature thick, tapering distally without reaching the tail tip. Lateral lines not visible. Oral disc (Fig. 2B) mid-sized (41% of maximum width of body), ventral, scarcely pigmented, and emarginated; marginal papillae in a single row, with wide dorsal and ventral gaps (83% and 51% of oral disc width, respectively); submarginal papillae scarce (1–3), on the upper and also frequently on the lower commissure; jaw sheaths darkly colored, serrated, and with similar width, the upper sheath gently curved with distal ends oriented posterolaterally, and the lower sheath smaller and V-shaped. Labial tooth row formula 2(2)/3; gap in A2 row 5–10 teeth wide, P1 and P3 slightly shorter than P2; labial teeth are curved, with a wide sheath, scarcely marked neck, and head with 10–12 marginal cusps (Fig. 4B). Coloration: in preserved specimens, dorsum and lateral sides of the body light brown, venter translucent with a few melanophores scattered on the gular region. A dark, straight dorsal line (which in early embryos points out the distribution of cells of the hatching gland) still visible at the analyzed stages, from the nares level to the otic region. Tail musculature lighter; fins mostly unpigmented, excepting a narrow band at the fin-muscle junction.

Rhinella vellardi.—(Figs. 1C, 2C; *n* = 2, stage 37) Body slightly depressed and oval from dorsal view; maximum width at the otic region. Snout widely truncate in dorsal view and rounded in lateral view. Ventral body contour slightly convex in the abdomen. Nostrils large (5% of maximum width of body), dorsal, rounded, with a slightly elevated rim and a barely outlined medial projection; nostrils closer to the tip of the snout than to the eyes. Eyes large (19% of maximum width of body) and dorsolateral. Pineal end organ not visible. Spiracle sinistral and placed at the middle third of the body, short, conical, posterodorsally oriented; external wall slightly folded dorsal and ventrally, giving an appearance of spiracle free from the body wall, but

inner wall absent; small oval opening with its major axis oriented dorsoventrally. Gut switchback point medial or slightly displaced to the left of the abdominal cavity. Vent tube short and cylindrical, directed medially and opened dextral, margin fused to the ventral fin. Tail 1.5 larger than the body, with maximum height at half its length; dorsal fin originating at the body-tail junction, with the first portion low and almost parallel to the longitudinal body axis and then abruptly curved and taller; ventral fin lower than the dorsal fin and uniformly high; tail tip narrowly rounded. Tail taller than the body (ratio between body maximum height and maximum tail height is about 0.8). Caudal musculature thick, tapering distally without reaching the tail tip. Lateral lines not visible. Oral disc (Fig. 2C) mid-sized (37% of the body width), ventral, scarcely pigmented, and emarginated; marginal papillae in a single row, with wide dorsal and ventral gaps (81% and 57% of oral disc width, respectively); submarginal papillae scarce (1–3) on both commissures; jaw sheaths darkly colored, serrated, and with similar width, the upper sheath gently curved with distal ends oriented posterolaterally, and the lower sheath smaller and V-shaped. Labial tooth row formula 2(2)/3; gap in A2 row about 10 teeth wide, P3 slightly shorter than P2; labial teeth are curved, with a wide sheath, scarcely marked neck, and head with 12–14 marginal cusps (Fig. 4G). Coloration: in preserved specimens, dorsum and lateral sides of the body light brown, venter translucent with a few melanophores scattered on the gular and branchial regions. Dark dorsal line outlined between the nares and the otic region. Tail musculature lighter with several unpigmented spots; fins mostly unpigmented, excepting a narrow band at the fin-muscle junction.

Tadpoles of *Rhinella altiperuviana*, *R. limensis*, *R. papillosa*, *R. spinulosa*, *R. trifolium*, and the two populations of *R.* aff. *spinulosa* were pictured in Figure 3. All tadpoles had labial tooth row formula (LTRF) 2(2)/3, excepting some specimens of *R. altiperuviana* (3 of 16

tadpoles examined) and *R. trifolium* (2 of 29) that showed LTRF 2(2)/3(1). Submarginal papillae were absent or scarce (1–3) and frequently arranged only in the upper commissures, excepting *R. limensis* where all specimens analyzed had papillae on both commissures. Main variations included body shape and the length of the gap in row A2. Tadpoles of *R. limensis* had a globose body shape, with high tail fins taller than the body (ratio between body maximum height and maximum tail height about 0.9); the row A2 in these tadpoles showed a very short gap, about 4–5 teeth wide. Conversely, tadpoles of *R. altiperuviana*, *R. papillosa*, *R. spinulosa*, *R. trifolium*, and *R.* aff. *spinulosa* were more streamlined with lower fins (ratio between body maximum height and maximum tail height 1–1.26), body highly pigmented, and the gap in A2 was much longer, about 15–30 teeth wide. Labial teeth were similar in all these taxa (Fig. 4). Lateral lines were usually not evident. The exceptions were *R.* aff. *spinulosa* MZA, where all lines were visible without staining, *R. altiperuviana* and *R. papillosa* with dorsal lines evident but ventral lines diffuse, and some specimens of *R. trifolium* where dorsal and some ventral lines were visible. Lateral lines of *R.* aff. *spinulosa* MZA were pictured in Figure 5 and arranged as follows. The dorsal line extended between the midbody, at the level of the origin of the epaxial musculature, and the first third of the dorsal fin. The medial line originated slightly anterior to the dorsal line and ran ventral and parallel through the caudal muscles; it described a wide curve and returned to the dorsal margin of the musculature to almost reach the tip of the tail. The ventral line originated in a medial point in the abdominal region, ran transversely to the side of the body and then directed caudally to end in a region anterior to the limb base; on the left side it was interrupted at the spiracle level. The angular line ran transversely between a ventral point next to the peribranchial wall level and a region below the eye. Four lines originated around the oral disc. The longitudinal oral line originated dorsolateral to the disc and ran caudally for a short tract reaching the eye level; in some specimens it joined the angular line. The oral line began lateral to

the disc and ran ventral and caudally through the gular region, up to the level of the peribranchial wall; in some specimens this line diverged from the longitudinal oral line. The supraorbital line originated dorsal to the oral disc and ran medial to the nares reaching the posterior margin of the eye. The infraorbital line in turn began dorsolateral to the disc and directed longitudinally below the eye up to its posterior margin. A short postsupraorbital line occurred caudal to the supraorbital line, in some specimens diverging from its posterior edge. Likewise, a very short postinfraorbital line appeared below and posterior to the infraorbital line. Finally, in some specimens an extra line ran longitudinally between the infraorbital and longitudinal oral lines.

Buccopharyngeal Cavity

The buccal cavity of tadpoles of *Rhinella altiperuviana* was described by Vera Candioti (2007; as *Chaunus spinulosus*) and some features of the buccal cavity of *R. limensis* tadpoles were described by Aguilar and Pacheco (2005; as *Bufo limensis*). In the paragraphs below we described comparatively features of all tadpoles examined in this work. Figures 6 and 7 showed the general aspects and some morphological variations.

On the buccal roof (Figs. 6A, 7A–C), the prenarial arena showed 1–5 pustulations arranged transversely (*Rhinella achalensis*, *R. altiperuviana*, *R. gallardoi*, *R. spinulosa*, *R. trifolium*, *R.* aff. *spinulosa*, and some specimens of *R. limensis*) or a transverse ridge (in *R. papillosa*, *R. vellardi*, and some specimens of *R. limensis*). The choanae were large and arranged obliquely at an angle of about 45º from the longitudinal axis; the anterior margin had small prenarial papillae, and the narial valve was smooth and thick. Three to five paired postnarial papillae were arranged in an inverted V-shape; they were simple and conical, and the second pair was usually the largest; small pustulations were scattered among these papillae. The lateral ridge papillae were well developed, flat, wide, and branched with 2–4 pustulate tips. The median ridge

was marginally ornamented and varied in shape, including high triangular (in *R. achalensis*, *R. limensis*, *R. papillosa*, *R. trifolium*, *R. vellardi*, and *R.* aff. *spinulosa* CAT) and rectangular (in *R. altiperuviana*, *R. gallardoi*, *R. spinulosa*, and *R.* aff. *spinulosa* MZA). The buccal roof arena was defined by 3–5 pairs of papillae, conical or bifurcate; a group of 2–3 papillae or small pustulations diverged laterally from the caudal edge of the arena, parallel to the glandular zone in all species but *R. gallardoi*, *R. trifolium*, and *R. vellardi*. Small pustulations and low papillae were scattered on the buccal roof arena and between roof papillae. The glandular zone was evident in all species, with large secretory pits disposed in a wide U-shaped arrangement. The dorsal velum was short, medially interrupted, smooth (in *R. achalensis*, *R. papillosa*, *R. vellardi*, and *R.* aff. *spinulosa* MZA) or with small marginal papillae (in *R. atiperuviana*, *R. gallardoi*, *R. limensis*, *R. spinulosa*, *R. trifolium*, and *R.* aff. *spinulosa* CAT).

On the buccal floor (Figs. 6B, 7D–F), non-keratinized spurs occurred at the edges of the lower jaw sheath, with curved, medially oriented tips, sometimes bifurcate (*Rhinella achalensis* and *R. spinulosa*). Paired infralabial papillae were placed on the internal surface of Meckel's cartilage and were wide, flap-like, flat, with 3–4 rounded tips oriented anteriorly; in most specimens a few very small pustulations arranged transversely on the internal aspect of the infrarostral cartilages. On the tongue anlage, four lingual papillae were conical (excepting in the examined specimens of *R. papillosa*, *R. trifolium*, and *R. vellardi* where some were bifid) and tall; laterally, tadpoles of *R. gallardoi*, *R. limensis*, *R. vellardi*, and *R.* aff. *spinulosa* CAT showed two rounded lingual pads. The buccal floor arena was delimited on both sides by 8–10 pairs of tall, mostly conical papillae; the papillae nearest to the buccal pockets were the largest and often flat and deeply branched. Several pustulations and low papillae were scattered on the arena and among main papillae. Groups of 3–6 prepocket papillae diverged laterally along the anterior margin of the buccal pockets, and caudally, 3–6 small papillae diverged laterally delimiting the

anterior edge of the ventral velum. The buccal pockets were elongated and arranged oblique. The ventral velum was semicircular and supported by spicules. Main marginal projections appeared on each side over filter plates, and at the midline where a median notch was absent; the margin was gently undulated in the remaining regions. Secretory pits develop on the ventral margin of the velum, and are mainly noticeable in specimens of *R. altiperuviana* and the two populations of *R.* aff. *spinulosa*.

Cranial Skeleton

Aspects of larval cranial skeleton were described only in *Rhinella altiperuviana* (Vera Candioti 2007; as *Chaunus spinulosus*). In the paragraphs below we summarized morphological variations in all species examined (Figs. 8, 9).

The neurocranium was almost as wide as long, dorsoventrally flattened, and mostly open dorsally (Figs. 8A,E, 9A–D). The suprarostral cartilage (Figs. 8B,F, 9E,F) had a single, U-shaped medial element dorsally fused to the lateral alae; corpora cartilages appeared comparatively thinner in *Rhinella limensis* and *R. vellardi*. Each ala was triangular and had well-developed dorsal anterior and posterior processes. In some specimens of *R. achalensis*, *R. altiperuviana*, *R. gallardoi*, and *R. spinulosa* the suprarostrals showed a narrow proximal connection between ala and corpus. The trabecular horns represented about 23% of the chondrocranial length, and they diverged describing an angle of 60º in average; the anterior margins were slightly expanded, and a small lateral trabecular process projected on the ventrolateral margin in all specimens except for *R. vellardi*. In the ethmoid region, the nasal septum and lamina orbitonasales were outlined in all species excepting *R. limensis*. The orbital cartilages were weak and low with an irregular dorsal margin. The taeniae tecti marginales were slightly chondrified and did not reach the anterior margin of the otic capsules. The optic and oculomotor foramina were defined on the posterior

ends of the cartilage, and the prootic fissure was visible and open dorsally. The large pituitary fenestra was covered by a sheet of chondrified tissue but the carotid foramen was not always completely encircled by cartilage (e.g., in specimens of *R. gallardoi*). The otic capsules were rhomboidal structures that corresponded to about to 27% the of chondrocranial length; the major axis of each capsule was almost parallel to the chondrocranium longitudinal axis. The fenestra ovalis occurred ventrally and the operculum was not yet developed; the jugular and inferior perilymphatic foramina were visible. The otic capsules were fused to the basicranial floor; they connected to each other dorsally by a thin chondrified tectum synoticum; they showed a thin crista parotica in all species, but a small and pointed anterolateral process was evident only in *R. achalensis*, *R. altiperuviana*, *R. spinulosa*, and *R. trifolium*.

The palatoquadrate arranged slightly divergent anteroposteriorly from the chondrocranium longitudinal axis. The articular process was long and wider than the rest of the cartilage; the anterior margin, which articulated with the Meckel's cartilage, was smooth, and a long, thin quadratoethmoid process projected from the medial margin. The muscular process was wide and rounded, and a thick quadratoorbitalis commissure extended between its tip and the base of the quadratoethmoid process. The pseudopterygoid process was absent. The subocular bar expanded posteriorly at the level of the ascending process; the posterior region was concave, with a posterolateral margin angular (more evident in *Rhinella achalensis, R. altiperuviana, R. spinulosa*, and *R. trifolium*) or rounded (as in *R. gallardoi* and *R. limensis*), and it showed a thick, dorsal edge that was continuous with the ascending process; a pointed otic process was evident at the posterolateral corner in *R. achalensis*, *R. spinulosa*, and *R. trifolium*. The ascending process was thin and attached almost perpendicularly to the chondrocranium in an intermediate attachment. The larval otic process was absent (excepting a unilateral process in the analyzed specimen of *R. vellardi*). The fenestra subocularis extended for about 27% of the chondrocranial

length. In the lower jaw (Fig. 8C,G), Meckel's cartilages were slightly curved, with a dorsolateral edge rounded and a robust retroarticular process; the medial edge had ventromedial and dorsomedial processes. The infrarostral cartilages were paired, thin, and connected medially through an alcianophilic symphysis.

In the hyobranchial skeleton (Fig. 8D,H), the ceratohyals were strongly chondrified and had five tall, robust processes. The anterior processes were triangular and oriented slightly lateral; the anterolateral processes were wider, lower, and oriented medially. The posterior processes had a wide base, and their tips diverge slightly lateral contacting the hypobranchial plate. On the lateral edge of the ceratohyals, small lateral processes projected from the anterior margin, and stout articular condyles were seen on the dorsal surface. The pars reuniens joining the ceratohyals was quadrangular, wide, and formed of a different type of cartilage (Fig. 9G); the basibranchial was narrower and shorter, fused to the hypobranchial plate, and had a long, square urobranchial process. The basihyal was absent. The hypobranchial plates were flat and articulate medially leaving a large triangular notch at the posterior region. The four pairs of ceratobranchials were long, thin, and curved, with numerous marginal projections. Ceratobranchials I and II were fused to the hypobranchial plate and had branchial processes; in some specimens of *Rhinella achalensis* a branchial process III was outlined. In most specimens (excepting *R. trifolium*) ceratobranchial III articulated with the hypobranchial plate through a syndesmotic union. Ceratobranchial IV was not attached to the plate. The ceratobranchials were connected posteriorly by thin terminal commissures; proximal commissures and branchial bridges between ceratobranchials were absent. Dorsally, four long, curved spicules were present, but the fourth was usually very weak and not connected to the ceratobranchial IV; in *R. altiperuviana* and *R. trifolium* there was a cartilaginous bridge joining spicules III and IV (Fig. 9H).

No cranial ossifications were present at the stages analyzed in most species, excepting frontoparietals, parasphenoid, and exoccipitals that occur in individuals of *Rhinella spinulosa* (Fig. 9A). Subhyoid ligament was evident in all specimens, on the ventral surface of the ceratohyals (Fig. 10B).

Musculature

Larval musculature was previously described for *Rhinella altiperuviana* (Vera Candioti 2007; as *Chaunus spinulosus*). Muscle configuration was almost identical in all species analyzed, and followed the same pattern already known in other bufonids. Typical features were the m. subarcualis rectus I with three slips, the m. subarcualis rectus II-IV with fibers invading the third branchial septum, the presence of all seven mm. levatores mandibulae, and the absence of mm. mandibulolabialis superior, interhyoideus posterior, diaphragmatopraecordialis, and constrictor and dilatator laryngis. Table 2 summarized descriptions of the 31 muscles as seen in *R. achalensis*, and Figure 10 illustrated some distinct features in the genus. Minor variations in other species were commented in the lines following. Medial and ventral slips of the m. srI were not well defined in *R. limensis* and *R. trifolium*. The lateral fibers of the m. srII-IV ran for half the ceratobranchial IV length in *R. limensis*. In *R. papillosa* specimens, some caudal fibers of the m. subarcualis obliquus inserted on ceratobranchial III. Subhyoid ligament was not well-developed in *R. limensis*, and fibers of the m. rectus abdominis did not reach it. Finally, a very poorly developed, almost indistinguishable m. dilatator laryngis appeared in one specimen of *R. trifolium*.

DISCUSSION

379 Comparative studies have coincided when highlighting the conservative larval
380 morphology in bufonids (e.g., Haas 2003). Within *Rhinella*, excepting some clades with distinct
381 features (such as the *R. veraguensis* and *R. granulosa* groups; Blotto et al. 2014; Haad et al. 2014;
382 Grosso et al., in press), the intrageneric groups apparently lack diagnostic larval traits. In our
383 study considering almost all tadpoles now assigned to the *Rhinella spinulosa* group, we found no
384 diagnostic features for the clade, but two distinct morphs among species. Most tadpoles are
385 highly pigmented and slender, with low tail fins lower or as high as the body, and their oral
386 morphology shows a long gap in the second anterior labial tooth row. This morphology is typical
387 of tadpoles of *R. achalensis*, *R. altiperuviana*, *R. papillosa*, *R. spinulosa, R. trifolium*, and the two
388 populations of *R.* aff. *spinulosa*. Conversely, tadpoles of *R. limensis* and *R. vellardi* share a
389 globose body morphology, high tail fins and a very short gap in tooth row A2. In turn, tadpoles of
390 *R. gallardoi* have a combination of streamlined body and A2 gap with intermediate length. The
391 original assigning of this species to the *R. veraguensis* group (Carrizo 1992) was not supported
392 by larval morphology, since known tadpoles of this group show a set of distinct external and
393 internal features (e.g., undivided row A2, gular depression or abdominal sucker, adrostral
394 cartilages; Aguayo et al. 2009; Haad et al. 2014), none of which are present in *R. gallardoi*.
395 While the distinction of two morphs in body shape within the *Rhinella spinulosa* gr. was
396 not discussed in previous literature, variations in the length of the gap in A2 row were already
397 noticed by Aguilar and collaborators when comparing tadpoles of *R. limensis* with other Peruvian
398 larvae (Angulo and Aguilar 2003; Aguilar and Gamarra 2004; Aguilar et al. 2007a). Interpreting
399 these two characters and their relationship along the phylogenetic hypothesis for the *R. spinulosa*
400 gr. (M. O. Pereyra, personal observation) shows that the globose morph could define the clade
401 composed of *R. limensis* and *R. vellardi*, and that the slender morph characterizes the large clade

including all the remaining species. A long gap in row A2 would have evolved within this latter, in the clade joining all species but *R. gallardoi*.

The oral discs vary slightly in other features as well. These variations are not unambiguously related to the said morphs, and should be checked in wider samples to interpret their distribution. For instance, a small gap in row P1 appeared in 20% of the analyzed specimens of *Rhinella altiperuviana*, and was reported in tadpoles of *R. trifolium* (Sinsch 1986), 20% of *R. limensis* studied by Angulo and Aguilar (2003), and all *R. limensis* studied by Aguilar and Gamarra (2004). In addition, submarginal papillae were scarce and mostly on the upper commissure in tadpoles with slender morphology, whereas they occurred also in the lower commissure in all the examined globose tadpoles (see also Angulo and Aguilar 2003; Aguilar et al. 2007a) and in some specimens of *R.* aff. *spinulosa* (Fernández 1927; Cei 1980). Larval measurements were very similar interspecifically, excepting the aforementioned differences in tail and body heights, and an outlined discrimination in naris relative size and position (slightly larger, caudal, and more distant to each other in slender tadpoles).

The ecological significance of variations in traits discussed, if any, should be further explored. On one hand, a streamlined body shape is frequent in anuran larvae from lotic environments (e.g., Altig and McDiarmid 1999), including related (e.g., species of the *R. veraguensis* group, *Nannophryne cophotis*; Aguilar and Gamarra 2004; Aguayo et al. 2009) and unrelated Andean tadpoles (e.g., *Telmatobius atahualpai*; Aguilar et al. 2007b). However, all tadpoles of *R. spinulosa* group, irrespective of their morphotype, develop in similar water bodies, in general shallow pools and slow-moving rivulets at margins of streams. Additionally, tadpoles with the globose morph inhabit different environments, with *R. limensis* restricted to Peruvian coastal deserts and *R. vellardi* distributed in dry forests at higher elevations (Cei 1972). In this scenario, it seems likely that if an ecomorphological correlation between body shape and type of

environment occurred, it was early during the evolution of the *R. spinulosa* group, and later diversification allowed for different phenotypes to appear and persist in those same environments. On the other hand, the loss of labial teeth (naturally occurring, in tadpoles affected by pathogens, or after surgery removal) has functional consequences in oral disc kinematics compromising feeding efficiency (Venesky et al. 2010a,b,c). While the differences in length of the gaps in the A2 tooth row of slender vs. globose tadpoles would appear to be too subtle, slight variations in the anchoring of tooth ridges to substrates during foraging cannot be ruled out.

Available information on internal morphology of tadpoles of the *Rhinella spinulosa* group is scarce. Some buccopharyngeal traits were mentioned in *R. limensis* (Aguilar and Pacheco 2005), and morphology of the buccal cavity and musculoskeletal system were described in larvae of *R. altiperuviana* (Vera Candioti 2007). Rodrigues de Oliveira et al. (2013) studied comparatively buccal features of 12 *Rhinella* species of several intrageneric groups, and their data allowed for identifying general aspects and some interspecific comparisons. Tadpoles of the *Rhinella spinulosa* group share with most congeneric species the ornamentation of the prenarial arena, a single pair of infralabial papillae, and four lingual papillae. As noted by Rodrigues de Oliveira et al. (2013), in general infralabial papillae are branched in a distinct way, so that a deep, U-shaped notch bifurcates each papilla leaving uneven halves with secondary projections. In addition, in all tadpoles studied here the skin that covers the distal edges of the infrarostral cartilages folds in a particular manner defining a pair of pointed, curved projections medially oriented. These projections were referred as non-keratinized spurs by Vera Candioti (2007) and Kolenc et al. (2013) in some *Rhinella* tadpoles, but were not mentioned in descriptions of larvae of the *R. veraguensis* group (Aguayo et al. 2009; Haad et al. 2014). A re-examination of *R. quechua* and *R. rumbolli* tadpoles revealed very small projections, and scanning electronic micrographs of *R. abei*, *R. icterica*, and *R. ornata* in Rodrigues de Oliveira et al. (2013) also

showed them, suggesting that this is a feature universally present in the genus. Unlike in other clades (hylid *Scinax*, ranid *Hoplobatrachus*; Grosjean et al. 2004; Alcalde et al. 2011), the spurs are never keratinized in *Rhinella* tadpoles.

Variable buccal features in the genus include the presence and number of infrarostral ornamentation, shape of lingual papillae, extent of papillation of buccal arenas, shape of the median ridge, and configuration of the dorsal and ventral vela (see Tables in Rodrigues de Oliveira et al. 2013). Lingual papillae are in general simple and conical, but Y-shaped papillae appear in tadpoles of *Rhinella icterica*, *R. ornata*, *R. pombali*, *R. diptycha*, two species of the *R. granulosa* group (Rodrigues de Oliveira et al. 2013), and specimens of *R. papillosa* and *R. vellardi* here studied. Finally, most tadpoles of the *R. spinulosa* group (excepting the specimens of *R. gallardoi*, *R. trifolium*, and *R. vellardi*) have a line of buccal roof arena papillae or pustulations that diverge laterally parallel to the anterior margin of the glandular zone. These are evident in other *Rhinella* tadpoles (e.g., *R. abei*, *R. crucifer*, *R. icterica*), but further observations with wider samples would confirm whether they are not intraspecifically variable.

With the exception of larvae of the *Rhinella veraguensis* group that show several distinct features (e.g., adrostral cartilages, oblique ascending processes, short and wide articular processes; revised in Haad et al. 2014), the general aspect of the chondrocrania and hyobranchial skeleton is similar among *Rhinella* tadpoles (e.g., Vera Candioti 2007; Kolenc et al. 2013; Rodrigues de Oliveira et al. 2014). Shared features are the tripartite suprarostral cartilages, quadratoethmoid and lateral trabecular processes present, perpendicular ascending processes, quadratoorbital commissures present, and larval otic process absent. Slight variations, apparently not related to intrageneric groups, are the presence of anterolateral processes of the crista parotica (in *R. diptycha*, *R. granulosa*, and within the *R. spinulosa* group, in *R. achalensis*, *R. altiperuviana*, *R. spinulosa*, and *R. trifolium*), cartilaginous bridges between suprarostral corpus

and alae (in *R. achalensis*, *R. altiperuviana*, *R. gallardoi*, and *R. spinulosa*), and small palatoquadrate otic processes (in *R. achalensis*, *R. spinulosa*, and *R. trifolium*). Likewise, muscular characters are highly conserved in *Rhinella* and bufonids in general, and the two synapomorphies recovered by Haas (2003) for the family (i.e., m. diaphragmatopraecordialis absent and m. subarcualis rectus II–IV with a lateral, diverging slip) occur in all species of the *R. spinulosa* group. Laryngeal muscles are absent in almost all tadpoles examined here. Although the distribution of these muscles was not analyzed in a phylogenetic context, data on other genera (e.g., *Melanophryniscus*; Baldo et al. 2014) suggested a widespread absence or deep reduction of mm. constrictor et dilatator larynges that could be related to the general reduction and late development of lungs in bufonid tadpoles (Haas 2003). Finally, the configuration of the m. rectus abdominis, with medial slips reaching or overpassing the branchial region, seems to be similar in *Rhinella* tadpoles described; some differences in myotome thickness and packing of fibers could be revealed after detailed quantification, at least regarding tadpoles of the *R. granulosa* group (F. Vera Candioti, personal observation).

Finally, three species formerly assigned to the *Rhinella spinulosa* group, *R. arunco*, *R. atacamensis*, and *R. rubropunctata*, were excluded from the group (M. O. Pereyra, personal observation). Larval external morphology in all of them shows features that are similar to those of the *R. gallardoi* + *R. spinulosa* clade (i.e., a rather slender body and A2 gap mid-sized to long; Cei 1962; Formas and Pugín 1978), but a thorough examination and coding in these and other related *Rhinella* would be required to assess phylogenetic status for these features.

Acknowledgments.—We are grateful to J. Faivovich, S.J. Nenda, and B.L. Blotto (MACN); and P.J. Torres (LGE) for access to collections and institutional specimen loans. We also deeply thank P.J. Venegas (CORBIDI) who provided us the tadpoles of *Rhinella vellardi*. This work was supported by Agencia Nacional de Promoción Científica y Tecnológica (PICT

2015-0813, 2015-2381, 2017-2437, 2018-3349), and a fellowship to KST from the ELEVATE Irish Research Council-MSCA cofund program (ELEVATEPD/2014/69). We thank pertinent national and regional authorities for collecting permits. We thank three anonymous reviewers for their suggestions and corrections that greatly improved our work.

LITERATURE CITED

Aguayo, R., E.O. Lavilla, F. Vera Candioti and T. Camacho. 2009. Living in fast-flowing water: Morphology of the gastromyzophorous tadpole of the bufonid *Rhinella quechua* (*R. veraguensis* group). Journal of Morphology 270:1431–1442.

Aguilar, C., and R. Gamarra. 2004. Descripción de dos renacuajos y una clave para las larvas conocidas del grupo *Bufo spinulosus* (Anura: Bufonidae) de Perú. Revista Peruana de Biología 11:31–36.

Aguilar, C., and V. Pacheco. 2005. Contribución de la morfología bucofaríngea larval a la filogenia de *Batrachophrynus* y *Telmatobius*. Monografías de Herpetología 7:219–238.

Aguilar, C., M. Lundberg, K. Siu-Ting and M.E. Jiménez. 2007a. Nuevos registros para la herpetofauna del departamento de Lima, descripción del renacuajo de *Telmatobius rimac* Schmidt, 1954 (Anura: Ceratophrydae) y una clave de los anfibios. Revista Peruana de Biología 14:209–216.

Aguilar, C., K. Siu-Ting and P. Venegas. 2007b. The rheophilous tadpole of *Telmatobius atahualpai* Wiens, 1993 (Anura: Ceratophryidae). South American Journal of Herpetology 2:165–174.

Alcalde, L., F. Vera Candioti, F. Kolenc, C. Borteiro and D. Baldo. 2011. Cranial anatomy of tadpoles of five species of *Scinax* (Hylidae, Hylinae). Zootaxa 2787:19–36.

521 Altig, R. 2007. A primer for the morphology of anuran tadpoles. Herpetological Conservation
522 and Biology 2:71–74.
523 Altig, R., and R.W. McDiarmid. 1999. Body plan. Development and morphology. Pp. 24–51 in
524 Tadpoles: The Biology of Anuran Larvae (R.W. McDiarmid and R. Altig, eds.). The
525 University of Chicago Press, USA.
526 Angulo, A., and C. Aguilar. 2003. The tadpole of *Bufo limensis* (Werner, 1901) (Anura:
527 Bufonidae). Amphibia Reptilia 24:400–405.
528 Baldo, D., F. Vera Candioti, B. Haad, (…) and M.R. Pie. 2014. Comparative morphology of
529 pond, stream and phytotelm-dwelling tadpoles of the South American Redbelly Toads
530 (Anura: Bufonidae: *Melanophryniscus*). Biological Journal of the Linnean Society
531 112:417–441.
532 Blotto, B., M.O. Pereyra and D. Baldo. 2014. The tadpole of *Rhinella azarai* (Gallardo, 1965)
533 with comments on the larval morphology in the *Rhinella granulosa* species group (Anura:
534 Bufonidae). Journal of Herpetology 48:434–438.
535 Bock, W.J., and C.R. Shear. 1972. A staining method for gross dissection of vertebrate muscles.
536 Anatomischer Anzeiger 130:222–227.
537 Carrizo, G.R. 1992. Cuatro especies nuevas de anuros (Bufonidae: *Bufo* e Hylidae: *Hyla*) del
538 norte de la Argentina. Cuadernos de Herpetología 7:14–23.
539 Cei, J.M. 1960. Geographic variation of *Bufo spinulosus* in Chile. Herpetologica 16:243–250.
540 Cei, J.M. 1962. Batracios de Chile. Ediciones de la Universidad de Chile, Chile.
541 Cei, J.M. 1971. Análisis sero-inmunológico de diferentes niveles de especiación en *Bufo* del
542 grupo *spinulosus*. Acta Zoológica Lilloana 28:91–105.
543 Cei, J.M. 1972. *Bufo* of South America. Pp. 82–92 in Evolution in the Genus *Bufo* (W.F. Blair,
544 ed.). University of Texas Press, USA.

545 Cei, J.M. 1980. Amphibians of Argentina. Monitore Zoologico Italiano Monografia 2:1–609.
546 Córdova, J.H. 1999. On karyomorphs, cladistics and taxonomic status of the *Bufo spinulosus*
547 species group (Amphibia: Anura) in Peru. Stuttgarter Beiträge zur Naturkunde A
548 (Biologie) 600:1–28.
549 Duellman, W.E., and R. Schulte. 1992. Description of a new species of *Bufo* from northern Peru
550 with comments on phenetic groups of South American toads (Anura: Bufonidae). Copeia
551 1992:162–172.
552 Fernández, K. 1927. Sobre la biología y reproducción de batracios argentinos. Segunda parte.
553 Boletín de la Academia Nacional de Ciencias de Córdoba 29:271–328.
554 Formas, J.R., and E. Pugín. 1978. Tadpoles of *Hylorina sylvatica*, *Eupsophus vittatus*, and *Bufo*
555 *rubropunctatus* in southern Chile. Herpetologica 34:355–358.
556 Frost, D.R. 2019. Amphibian Species of the World: an Online Reference. Version 6.0 (Accessed
557 Dec 12 2019). Electronic Database accessible at
558 http://research.amnh.org/herpetology/amphibia/index.html. American Museum of Natural
559 History, New York, USA.
560 Gosner, K.L. 1960. A simplified table for staging anuran embryos and larvae, with notes on
561 identification. Herpetologica 16:183–190.
562 Grant, T., and W. Bolívar-G. 2014. A new species of semiarboreal toad with a salamander-like
563 ear (Anura: Bufonidae: *Rhinella*). Herpetologica 70:198–210.
564 Grosjean, S., M. Vences and A. Dubois. 2004. Evolutionary significance of oral morphology in
565 the carnivorous tadpoles of tiger frogs, genus *Hoplobatrachus* (Ranidae). Biological
566 Journal of the Linnean Society 81:171–181.

Grosso, J., M.O. Pereyra, F. Vera Candioti, N.M. Maciel and D. Baldo. Tadpoles of three species of the *Rhinella granulosa* group, with a reinterpretation of larval characters. In press in South American Journal of Herpetology.

Haad, M.B., F. Vera Candioti and D. Baldo. 2014. The stream tadpoles of *Rhinella rumbolli* (Anura: Bufonidae). Herpetologica 70:184–197.

Haas, A. 2003. Phylogeny of frogs as inferred from primarily larval characters (Amphibia: Anura). Cladistics 19:23–89.

Haas, W. 2002. Beitrag zum taxonomischen Status von *Bufo trifolium* Tschudi, 1845 und *Bufo spinulosus flavolineatus* Vellard, 1959 sowie zur Biologie von *Bufo spinulosus* Wiegmann, 1834. Salamandra 38:155–164.

Jetz, W., and R.A. Pyron. 2018. The interplay of past diversification and evolutionary isolation with present imperilment across the amphibian tree of life. Nature Ecology & Evolution 2:850–858.

Kolenc, F., C. Borteiro, L. Cotichelli, D. Baldo, C. Martínez Debat and F. Vera Candioti. 2013. The tadpole and karyotype of *Rhinella* (*Bufo*) *achavali* (Anura: Bufonidae). Journal of Herpetology 47:599–606.

Lannoo, M.J. 1987. Neuromast topography in anuran amphibians. Journal of Morphology 191:115–129.

Lavilla, E.O. 1983. Sistemática de Larvas de Telmatobiinae (Anura: Leptodactylidae). Doctoral thesis dissertation, Universidad Nacional de Tucumán, Argentina.

Moravec, J., E. Lehr, J.C. Cusi, J.H. Córdova and V. Gvoždík. 2014. A new species of the *Rhinella margaritifera* species group (Anura, Bufonidae) from the montane forest of the Selva Central, Peru. ZooKeys 371:35–56.

590 Pereyra, M.O., F. Vera Candioti, J. Faivovich and D. Baldo. 2015. Egg clutch structure of
591 *Rhinella rumbolli* (Anura: Bufonidae), a toad from the Yungas of Argentina, with a
592 review of the reproductive diversity in *Rhinella*. Salamandra 51:161–170.
593 Pramuk, J.B. 2006. Phylogeny of South American *Bufo* (Anura: Bufonidae) inferred from
594 combined evidence. Zoological Journal of the Linnean Society 146:407–452.
595 Pyron, R.A. 2014. Biogeographic analysis reveals ancient continental vicariance and recent
596 oceanic dispersal in amphibians. Systematic Biology 63:779–797.
597 Rodrigues de Oliveira, M.I.R., L.N. Weber and M.F. Napoli. 2013. Internal oral morphology in
598 larvae of the genus *Rhinella* Fitzinger, 1826 (Amphibia, Anura, Bufonidae). Zootaxa
599 3745:501–523.
600 Rodrigues de Oliveira, M.I.R., L.N. Weber and M.F. Napoli. 2014. Chondrocranial and
601 hyobranchial morphology in larvae of the genus *Rhinella* Fitzinger, 1826 (Amphibia,
602 Anura, Bufonidae). The Herpetological Journal 24:229–237.
603 Sinsch, U. 1986. Anfibios de la sierra central del Perú, una clave de identificación para adultos y
604 larvas. Boletín de Lima 45:23–33.
605 Van Bocxlaer, I., S.P. Loader, K. Roelants, S.D. Biju, M. Menegon and F. Bossuyt. 2010.
606 Gradual adaptation toward a range-expansion phenotype initiated the global radiation of
607 toads. Science 327:679–682.
608 Vellard, J. 1959. Estudios sobre batracios andinos V. El género *Bufo*. Memorias del Museo de
609 Historia Natural "Javier Prado" 8:1–48.
610 Venesky, M.D., R.J. Wassersug and M.J. Parris. 2010a. Fungal pathogen changes the feeding
611 kinematics of larval anurans. Journal of Parasitology 96:552–557.

612 Venesky, M.D., R.J. Wassersug and M.J. Parris. 2010b. How does a change in labial tooth row
613 number affect feeding kinematics and foraging performance of a ranid tadpole (*Lithobates*
614 *sphenocephalus*)? The Biological Bulletin 218:160–168.
615 Venesky, M.D., R.J. Wassersug and M.J. Parris. 2010c. The impact of variation in labial tooth
616 number on the feeding kinematics of tadpoles of Southern Leopard Frog (*Lithobates*
617 *sphenocephalus*). Copeia 2010:481–486.
618 Vera Candioti, M.F. 2007. Anatomy of anuran tadpoles from lentic water bodies: systematic
619 relevance and correlation with feeding habits. Zootaxa 1600:1–175.
620 Wassersug, R.J. 1976a. Oral morphology of anuran larvae: terminology and general description.
621 Occasional Papers of the Museum of Natural History, University of Kansas 48:1–23.
622 Wassersug, R.J. 1976b. A procedure for differential staining of cartilage and bone in whole
623 formalin fixed vertebrates. Stain Technology 51:131–134.

APPENDIX

Specimens Examined

Rhinella achalensis.—ARGENTINA: CÓRDOBA: Departamento San Alberto: Pampa de Achala, Puesto Cuello near to El Volcán, LGE 04235, *n* = 14, stages 32–36. Skeleton (6, 35–36); muscles (1, 34); buccal cavity (1, 34).

Rhinella altiperuviana.—ARGENTINA: JUJUY: Departamento Humahuaca: Chucalezna, Río Grande, Quebrada de Humahuaca, LGE 03871 and Departamento Susques: Susques, Salar de Olaroz, LGE 22111, *n* = 16, stages 35–38. Skeleton (4, 35); muscles (2, 35 and 36); buccal cavity (1, 37).

Rhinella gallardoi.—ARGENTINA: JUJUY: Departamento Doctor Manuel Belgrano: Tilquiza, LGE 09887, *n* = 11, stages 29–31. Skeleton (2, 31); muscles (1, 31); buccal cavity (1, 31).

Rhinella limensis.—PERÚ: LA LIBERTAD: Cajabamba, Sanagorán, LGE 22101 and LIMA: Provincia Huarochirí: Barba Blanca, LGE 22102, *n* = 5, stages 30–38. Skeleton (1, 33); muscles (2, 33 and 35); buccal cavity (1, 33).

Rhinella papillosa.—ARGENTINA: NEUQUÉN : Departamento Minas: Camalón, MACN 50401, *n* = 17, stages 30–31. Skeleton (2, 31); muscles (1, 31); buccal cavity (1, 31).

Rhinella spinulosa.—PERÚ: AREQUIPA: Provincia Arequipa: Sabandía, LGE 22103, *n* = 2, stages 37. Skeleton (1); muscles (2); buccal cavity (1).

Rhinella trifolium.—PERÚ: PASCO: Paucartambo, MUSM 17815–6, LGE 22104, *n* = 29, stages 30–34. Skeleton (2, 33); muscles (2, 34); buccal cavity (2, 34).

Rhinella vellardi.—PERÚ: AMAZONAS: Provincia Chachapoyas: Balsas, Quebrada Honda, LGE 22105, *n* = 2, stages 37. Skeleton (1); muscles (1); buccal cavity (1).

Rhinella aff. *spinulosa*.—ARGENTINA: CATAMARCA: Departamento Andalgalá: Capillitas, LGE 22112, *n* = 7, stages 31–38. Skeleton (1, 37); muscles (1, 37–38); buccal cavity (1, 37); MENDOZA: Departamento Malargüe: Ruta Provincial N° 226, on the way to Paso Vergara, margins of the Río Valenzuela, LGE 17106, *n* = 6, stages 35–38. Skeleton (2, 35); muscles (1, 37); buccal cavity (1, 37).

652 TABLE 1.—External morphology measurements, presented as average (standard deviation), in species of the *Rhinella spinulosa* group.
653 The two last columns correspond to populations of *R.* aff. *spinulosa* from Argentinean Provinces Catamarca and Mendoza (CAT and
654 MZA respectively).

	R. achalensis	*R. altiperuviana*	*R. gallardoi*	*R. limensis*	*R. papillosa*	*R. spinulosa*	*R. trifolium*	*R. vellardi*	*R.* CAT	*R.* MZA
	n = 8	*n* = 10	*n* = 10	*n* = 3	*n* = 10	*n* = 1	*n* = 10	*n* = 1	*n* = 7	*n* = 7
	stages 32–33	stages 36–37	stages 30–37	stages 30–37	stages 30–31	stage 36	stages 32–34	stage 36	stages 30–32	stages 35–37
Snout vent length	8.80 (0.39)	13.86 (0.78)	9.92 (1.03)	12.86 (0.80)	8.94 (0.29)	11.89	9.14 (0.71)	11.49	8.65 (0.47)	12.27 (1.70)
Maximum body height	3.98 (0.37)	6.60 (0.42)	4.66 (0.79)	6.55 (0.77)	4.69 (0.20)	5.82	4.36 (0.33)	5.23	4.41 (0.22)	5.84 (0.84)
Maximum body width	5.07 (0.41)	8.73 (0.74)	5.70 (0.92)	8.32 (0.54)	5.53 (0.22)	7.67	5.67 (0.35)	6.94	4.95 (0.22)	7.37 (1.05)
Body width at eyes	4.37 (0.24)	6.52 (0.47)	4.67 (0.60)	6.69 (0.29)	4.50 (0.17)	6.06	4.63 (0.30)	5.89	4.13 (0.30)	5.67 (0.77)
Body width at nares	3.01 (0.17)	4.66 (0.36)	3.25 (0.39)	4.60 (0.20)	3.18 (0.15)	4.29	2.91 (0.23)	3.89	2.80 (0.22)	4.08 (0.57)
Dorsal gap width	1.83 (0.12)	2.42 (0.16)	1.92 (0.13)	2.15 (0.10)	1.74 (0.07)	2.09	1.6 (0,11)	2.08	1.73 (0.16)	2.30 (0.26)
Eye diameter	1.01 (0.06)	1.28 (0.17)	0.95 (0.22)	1.33 (0.13)	0.91 (0.04)	1.20	1.06 (0.11)	1.35	0.92 (0.08)	1.21 (0.17)
Eye-nares distance	1.69 (0.08)	2.54 (0.14)	1.88 (0.12)	2.54 (0.21)	1.66 (0.09)	2.39	2.12 (0.10)	1.79	1.84 (0.13)	2.45 (1.00)
Extranarial distance	0.87 (0.05)	1.55 (0.14)	1.16 (0.32)	1.37 (0.06)	0.93 (0.06)	1.15	1.00 (0.10)	0.96	0.95 (0.06)	1.34 (0.23)
Extraorbital distance	3.09 (0.10)	4.46 (0.26)	2.88 (0.57)	4.52 (0.48)	2.90 (0.09)	3.90	3.33 (0,25)	3.80	2.92 (0.35)	4.09 (0.59)
Fronto-narial distance	0.57 (0.10)	1.01 (0.19)	0.70 (0.17)	0.84 (0.04)	0.83 (0.12)	0.86	0.72 (0,10)	0.65	0.58 (0.09)	1.19 (0.26)
Internarial distance	1.20 (0.09)	1.66 (0.13)	1.36 (0.07)	1.97 (0.17)	1.14 (0.04)	1.52	1.48 (0.08)	1.16	1.21 (0.13)	1.83 (0.74)
Interorbital distance	1.89 (0.26)	3.39 (0.21)	1.72 (0.55)	3.43 (0.28)	1.92 (0.13)	2.99	2.08 (0.14)	1.90	1.94 (0.18)	3.00 (0.40)

Maximum tail height	4.04 (0.30)	5.32 (0.35)	4.27 (0.70)	6.74 (0.70)	4.00 (0.16)	5.74	4.33 (0.25)	6.19	3.49 (0.28)	5.47 (0.79)
Naris length	0.33 (0.10)	0.50 (0.09)	0.38 (0.09)	0.50 (0.09)	0.37 (0.03)	0.59	0.5 (0.06)	0.35	0.44 (0.06)	0.55 (0.40)
Oral disc width	2.17 (0.12)	2.89 (0.20)	2.32 (0.17)	2.74 (0.27)	1.91 (0.08)	2.54	2.04 (0.09)	2.56	2.09 (0.16)	2.71 (0.19)
Rostro-spiracular distance	5.40 (0.19)	7.14 (0.62)	5.22 (0.65)	7.18 (0.64)	4.81 (0.31)	6.51	5.31 (0.48)	6.31	5.17 (0.27)	6.74 (0.93)
Tail length	14.14 (0.42)	21.88 (1.24)	15.14 (1.12)	20.10 (5.15)	12.38 (0.51)	18.37	14.84 (1.36)	16.98	13.74 (1.33)	19.00 (2.72)
Total length	22.94 (0.53)	35.85 (1.83)	24.02 (3.62)	26.26 (11.94)	20.44 (2.69)	30.25	23.98 (1.98)	30.25	20.13 (3.72)	28.91 (4.69)
Tail muscle height	1.65 (0.10)	2.62 (0.18)	2.07 (0.14)	3.07 (0.41)	1.57 (0.11)	2.86	1.84 (0.13)	2.11	1.91 (0.11)	2.47 (0.47)
Ventral gap width	1.27 (0.12)	1.62 (0.25)	1.19 (0.16)	1.60 (0.14)	1.01 (0.06)	1.12	0.95 (0.09)	1.45	1.22 (0.16)	1.75 (0.26)

655

656 TABLE 2.—Larval musculature in *Rhinella achalensis*.

Muscle	Attachments
Levator mandibulae longus superficialis	posterolateral margin of subocular bar – dorsomedial edge of Meckel's cartilage
Levator mandibulae longus profundus	posterolateral margin of subocular bar, ventral to levator mandibulae longus superficialis – frontal aspect of suprarostral ala, next to lateral margin, through a long, thin tendon
Levator mandibulae externus superficialis	medial point at the ascending margin of muscular process, at about half its length – posterior surface of the dorsolateral edge of suprarostral ala; ramus V3 is ventral to this muscle
Levator mandibulae externus profundus	inner surface of the ascending margin of muscular process, at about half its length – frontal surface of suprarostral ala, next to lateral margin, through a tendon common with that of levator mandibulae longus profundus
Levator mandibulae internus	ventral surface of the ascending process and anteroventral surface of the otic capsule – dorsolateral edge of Meckel's cartilage
Levator mandibulae articularis	inner surface of muscular process, ventral to levator mandibulae externus profundus –dorsolateral edge of Meckel's cartilage, medial to levator mandibulae

	internus
Levator mandibulae lateralis	lateral edge of articular process –dorsolateral edge of suprarostral ala
Mandibulolabialis	ventromedial edge of Meckel's cartilage – lower lip, in a small, mental area
Intermandibularis	ventrolateral edge of Meckel's cartilage – median aponeurosis attached to the ventral skin
Submentalis	ventral surface of infrarostral cartilages
Orbitohyoideus	dorsal edge of muscular process –lateral edge of ceratohyal
Suspensoriohyoideus	inferior region of the ascending margin of muscular process –posterolateral surface of the lateral edge of ceratohyal
Hyoangularis	dorsal surface of lateral process of ceratohyal – retroarticular process
Suspensorioangularis	ventral half of the descending margin of muscular process –posterolateral surface of the lateral edge of ceratohyal; it occupies the lower half of muscular process
Quadratoangularis	ventral surface of muscular process – retroarticular process
Interhyoideus	lateral edge of ceratohyal – median aponeurosis
Geniohyoideus	ventral surface of infrarostral – hypobranchial plate

	at the level of ceratobranchial III
Constrictor branchialis II	branchial process II – terminal commissure I; disposed on ceratobranchial I
Constrictor branchialis III	branchial process II – terminal commissure II; disposed on ceratobranchial II
Constrictor branchialis IV	branchial process II – distal edge of ceratobranchial III; disposed on ceratobranchial III
Levator arcuum branchialium I	lateral margin of subocular bar – lateral margin of ceratobranchial I
Levator arcuum branchialium II	posterolateral margin of subocular bar –terminal commissure I
Levator arcuum branchialium III	lateral and posterolateral margins of otic capsule – terminal commissure II; a posterior slip inserts more dorsally on the capsule
Levator arcuum branchialium IV	ventral surface of otic capsule – medial distal margin of ceratobranchial IV
Tympanopharyngeus	a few fibers that diverge medially from levator arcuum branchialium IV, to insert on the connective tissue anterior to glottis
Subarcualis rectus I	three slips originated at the posterior surface of the posterior process of the ceratohyal; ventral slip inserts on branchial process III, middle slip on branchial process II, and dorsal slip on proximal area

	of ceratobranchial I. The distinction between middle and ventral slips is not well defined at the insertion on ceratohyal
Subarcualis rectus II-IV	ceratobranchial II –lateral margin of proximal area of ceratobranchial IV; very thin. At the anterior insertion, some fibers are continuous with those of ceratobranchial II; at the posterior insertion, a thin slip diverges laterally following the ceratobranchial reaching its distal edge
Subarcualis obliquus	urobranchial process – branchial process II
Rectus cervicis	branchial process III – peribranchial peritoneum; short and thin
Diaphragmatobranchialis	distal edge of ceratobranchial III – peribranchial peritoneum; short and very thin
Rectus abdominalis	pelvic girdle – peritoneum. Lateral slips originate at the level of spiracle, and middle slips reach the pericardic region; more medial slips form a compact slip that continues as a fibrous connective tissue that reaches the subhyoid ligament, whereas the remaining medial fibers are loose and insert caudal and dorsally on the diaphragm

FIGURE CAPTIONS

FIG. 1.—The tadpoles of (A) *Rhinella achalensis* (stage 33, LGE 04235), (B) *R. gallardoi* (stage 31, LGE 09887), and (C) *R. vellardi* (stage 37, LGE 22105), showing lateral, dorsal, and ventral views. Scale bars = 1 mm.

FIG. 2.—Details of the oral discs of same specimens of (A) *Rhinella achalensis*, (B) *R. gallardoi*, and (C) *R. vellardi*. Scale bars = 0.5 mm.

FIG. 3.—Comparative external morphology in tadpoles of the *Rhinella spinulosa* group. Lateral views and detail of the oral disc are shown. (A) *R. altiperuviana* (stage 37, LGE 22111), (B) *R. limensis* (stage 34, LGE 22101), (C) *R. papillosa* (stage 31, MACN 50401), (D) *R. spinulosa* (stage 37, LGE 22103), (E) *R. trifolium* (stage 32, MUSM 17815–6), (F) *R.* aff. *spinulosa* CAT (stage 31, LGE 22112), (G) *R.* aff. *spinulosa* MZA (stage 38, LGE 17106). Scale bars = 1 mm. Note the two morphotypes differentiating the tadpoles of *R. limensis* (globose body and small gap in A2) vs. all the remaining tadpoles (slender bodies and larger gaps in A2).

FIG. 4.—Labial tooth morphology in tadpoles of the *Rhinella spinulosa* group, lateral views of individual teeth and details of head cusps. (A) *R. achalensis* (stage 33, LGE 04235), (B) *R. altiperuviana* (stage 37, LGE 22111), (C) *R. gallardoi* (stage 31, LGE 09887), (D) *R. limensis* (stage 34, LGE 22101), (E) *R. papillosa* (stage 31, MACN 50401), (F) *R. spinulosa* (stage 37, LGE 22103), (G) *R. trifolium* (stage 32, MUSM 17815–6), (H) *R. vellardi* (stage 37, LGE

22105), (I) *R.* aff. *spinulosa* CAT (stage 31, LGE 22112), (J) *R.* aff. *spinulosa* MZA (stage 38, LGE 17106). Scale bars, main divisions = 0.05 mm. Note the similar curved teeth with numerous marginal cusps.

FIG. 5.—Lateral lines, as seen in a tadpole of *Rhinella* aff. *spinulosa* MZA (stage 37, LGE 17106). AN = angular, D = dorsal, IO = infraorbital, LOR = longitudinal oral, M = median, OR = oral, PIO = postinfraorbital, PSO = postsupraorbital, SO = supraorbital, V = ventral.

FIG. 6.—Buccal roof (A) and floor (B) of *Rhinella achalensis* (stage 34, LGE 04235). BFAP = buccal floor arena papillae, BP = buccal pocket, BRAP = buccal roof arena papillae, DV = dorsal velum, GZ = glandular zone, ILP = papillae, IN = internal nare, LP = lingual papillae, LRP = lateral ridge papilla, MR = median ridge, PNA = prenarial arena, PPP = prepocket papillae, PTNP = postnarial papillae, S = spur, VV = ventral velum. Scale bars = 1 mm.

FIG. 7.—Details of buccal cavities of other species of the *Rhinella spinulosa* group, showing some distinctive features. Anterior region of the buccal roof of (A) *R. papillosa* (stage 31, MACN 50401) and (B) *R. spinulosa* (stage 37, LGE 22103); note the different shapes of the median ridges. (C) Posterior region of the buccal roof of *R. limensis* (stage 33, LGE 22102), showing the dorsal velum and glandular zone. (D) Anterior region of the buccal floor of *R. altiperuviana* (stage 37, LGE 22111), showing the spurs, infralabial and lingual papillae. (E) Detail of the tongue anlage of *R. gallardoi* (stage 31, LGE 09887), showing the lingual pads on

both sides of the tongue. (F) Detail of the buccal pockets of *R.* aff. *spinulosa* CAT (stage 37, LGE 22112), showing the prepocket papillae and general papillae of the floor arena. BFAP = buccal floor arena papillae, BP = buccal pocket, DV = dorsal velum, ILP = infralabial papillae, LP = lingual papillae, LRP = lateral ridge papilla, MR = median ridge, P = lingual pad, PPP = prepocket papillae, S = spur, SP = secretory pits. Scale bars = 1 mm.

FIG. 8.—Larval skeleton in *Rhinella achalensis* (stage 35, LGE 04235) and *R. gallardoi* (stage 31, LGE 09887). (A,E) Chondrocranium; (B,F) Suprarostral cartilage; (C,G). Lower jaw cartilages; (D,H) Hyobranchial skeleton. A = ala, AP = articular process, ASP = ascending process, C = corpus, CB = ceratobranchials, CH = ceratohyals, HP = hypobranchial plate, IR = infrarostral cartilage, LT = lateral trabecular process, MC = Meckel's cartilage, MP = muscular process, OC = otic capsule, PAL = anterolateral process of the otic capsule, PQ = palatoquadrate, PR = pars reuniens, QEP = quadratoethmoid process, QOC = quadratoorbital commissure, SB = subocular bar, TH = trabecular horns, TS = tectum synoticum. Scale bars = 0.5 mm. Chondrocrania are very similar, excepting the angular margin of subocular bar and the small anterolateral process of the otic capsules in *R. achalensis*.

FIG. 9.—Details of larval skeletons of other species of the *Rhinella spinulosa* group, showing some distinctive features (asterisks). Chondrocranium in (A) *R. spinulosa* (stage 37, LGE 22103), ventral view; note the small processes in the subocular bars and the otic capsules. (B) *R. papillosa* (stage 31, MACN 50401), ventral view; (C) *R.* aff. *spinulosa* MZA (stage 35, LGE 17106), dorsal view; note the pointed lateral trabecular processes in the two species. (D) *R.*

730 *vellardi* (stage 37, LGE 22105), ventral view; note the thin, unilateral larval otic process.
731 Suprarostral cartilages in frontal view of (E) *R. limensis* (stage 33, LGE 22102) and (F) *R.*
732 *spinulosa* (stage 37, LGE 22103); note the cartilaginous bridges between corpus and ala in the
733 latter. (G) Detail of pars reuniens of the specimen of *R. spinulosa,* showing the different type of
734 cartilaginous tissue. (H) Detail of four spicules in *R. altiperuviana* (stage 35, LGE 22111),
735 showing the cartilage bridge between spicules III and IV. Scale bars = 1 mm.
736
737
738 FIG. 10.—Larval cranial musculature in tadpoles of species of the *Rhinella spinulosa*
739 group. (A) Lateral view of the muscular process of *R. gallardoi* (stage 31, LGE 09887), showing
740 details of mm. levatores mandibulae; thin levator mandibulae lateralis and externus superficialis
741 are present in all species. (B) Ventral view of the mandibular region of *R.* aff. *spinulosa* CAT
742 (stage 37, LGE 22112), showing ventral muscles and the subhyoid ligament; when the ventral
743 skin is lifted, the attachment of the anterior portion of the m. intermandibularis to the lower lip
744 skin is evident. (C) Ventral view of the left branchial basket of *R. altiperuviana* (stage 35, LGE
745 22111), showing branchial muscles; note the lateral slip of the m. subarcualis rectus II-IV
746 invading the third branchial septum in a constrictor-like arrangement. (D) Detail of the left
747 branchial basket of *R.* aff. *spinulosa* MZA (stage 37, LGE 17106), showing the three slips of the
748 m. subarcualis rectus I. (E) Ventral view of the abdominal region of the specimen of *R. gallardoi*,
749 showing the general configuration of the m. rectus abdominis with three types of fibers. CBII-IV
750 = constrictor branchialis II-IV, GH = geniohyoideus, HA = hyoangularis, IM =
751 intermandibularis, LIG SH = subhyoid ligament, LMA = levator mandibulae articularis, LMEP =
752 levator mandibulae externus profundus, LMES = levator mandibulae externus superficialis, LML
753 = levator mandibulae lateralis, LMLS = levator mandibulae longus superficialis, MLI =

754 mandibulolabialis inferior, OH = orbitohyoideus, QA = quadratoangularis, RAL = rectus
755 abdominis lateral fibers, RAM1 = rectus abdominis medial, compact fibers, RAM2 = rectus
756 abdominis medial, loose fibers, SO = subarcualis obliquus, SRI = subarcualis rectus I, SRID =
757 subarcualis rectus I dorsal slip, SRII-IV = subarcualis rectus II-IV, SRIM = subarcualis rectus I
758 median slip, SRIV = subarcualis rectus I ventral slip, V3 = mandibular branch of the trigeminal
759 nerve. Scale bars = 0.5 mm excepting (E), 1 mm.

Figure 1

Click here to access/download;Figure;FIG1.tif

Figure 2

Click here to access/download;Figure;FIG2.tif

Figure 3

Click here to access/download;Figure;FIG3.tif

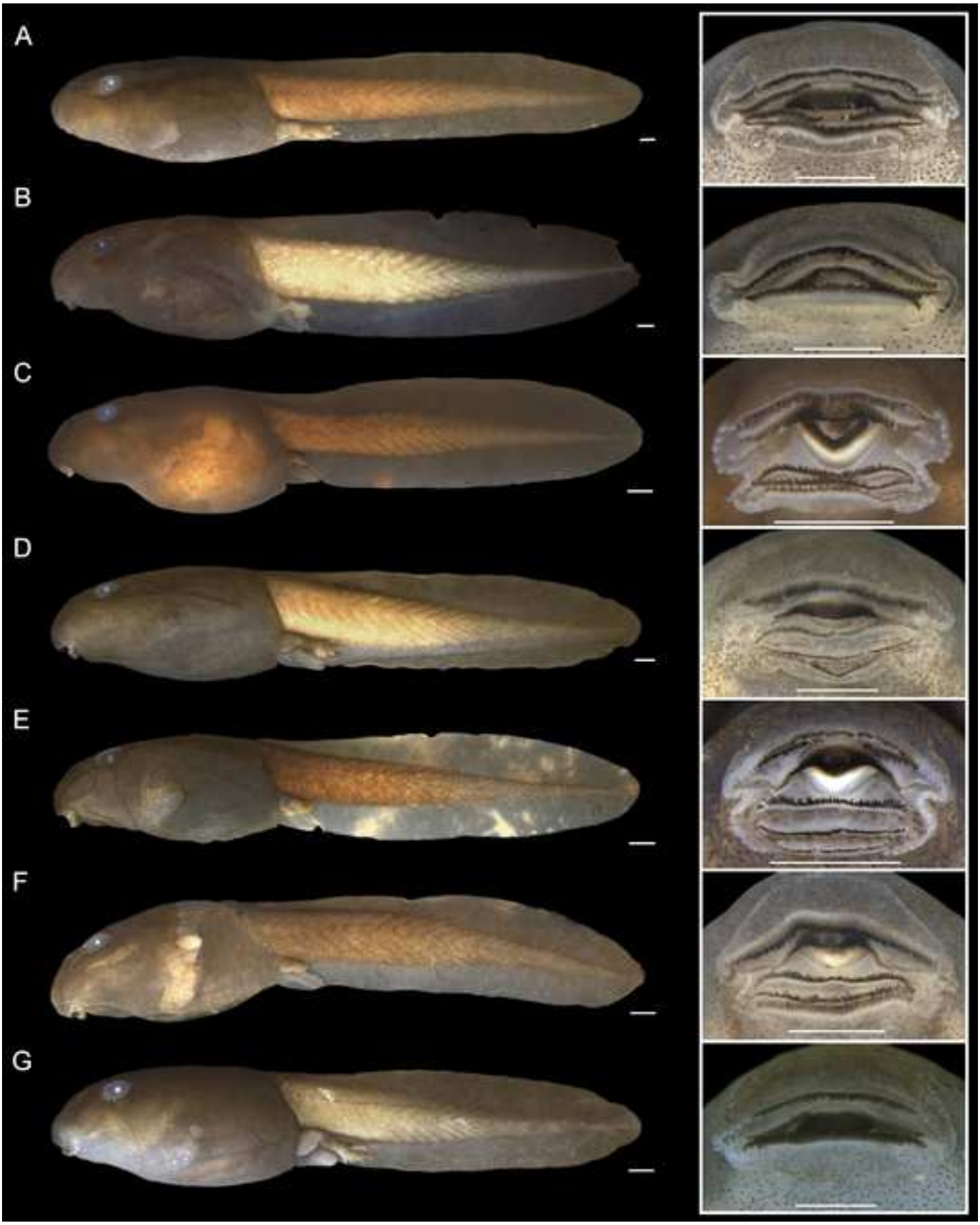

Figure 4

Click here to access/download;Figure;FIG4.tif

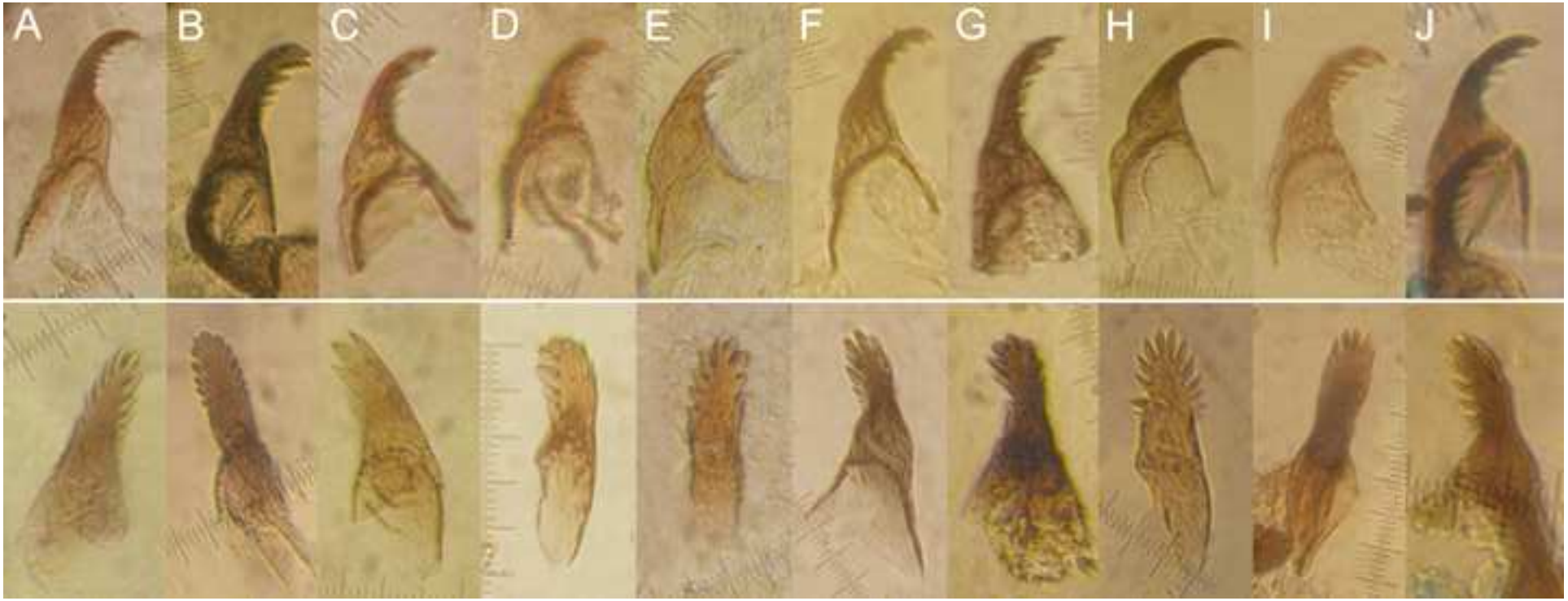

Figure 5

Click here to access/download;Figure;FIG5.tif

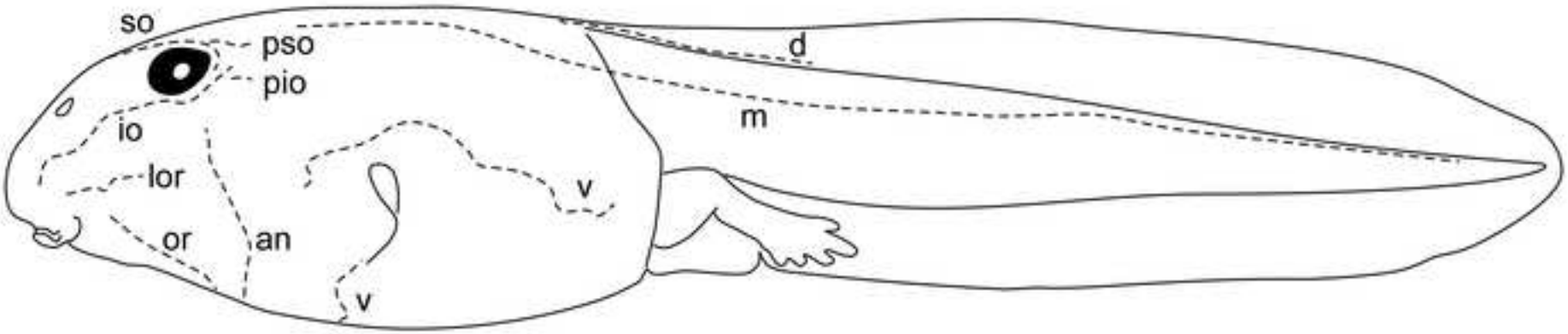

Figure 6

Click here to access/download;Figure;FIG6.tif

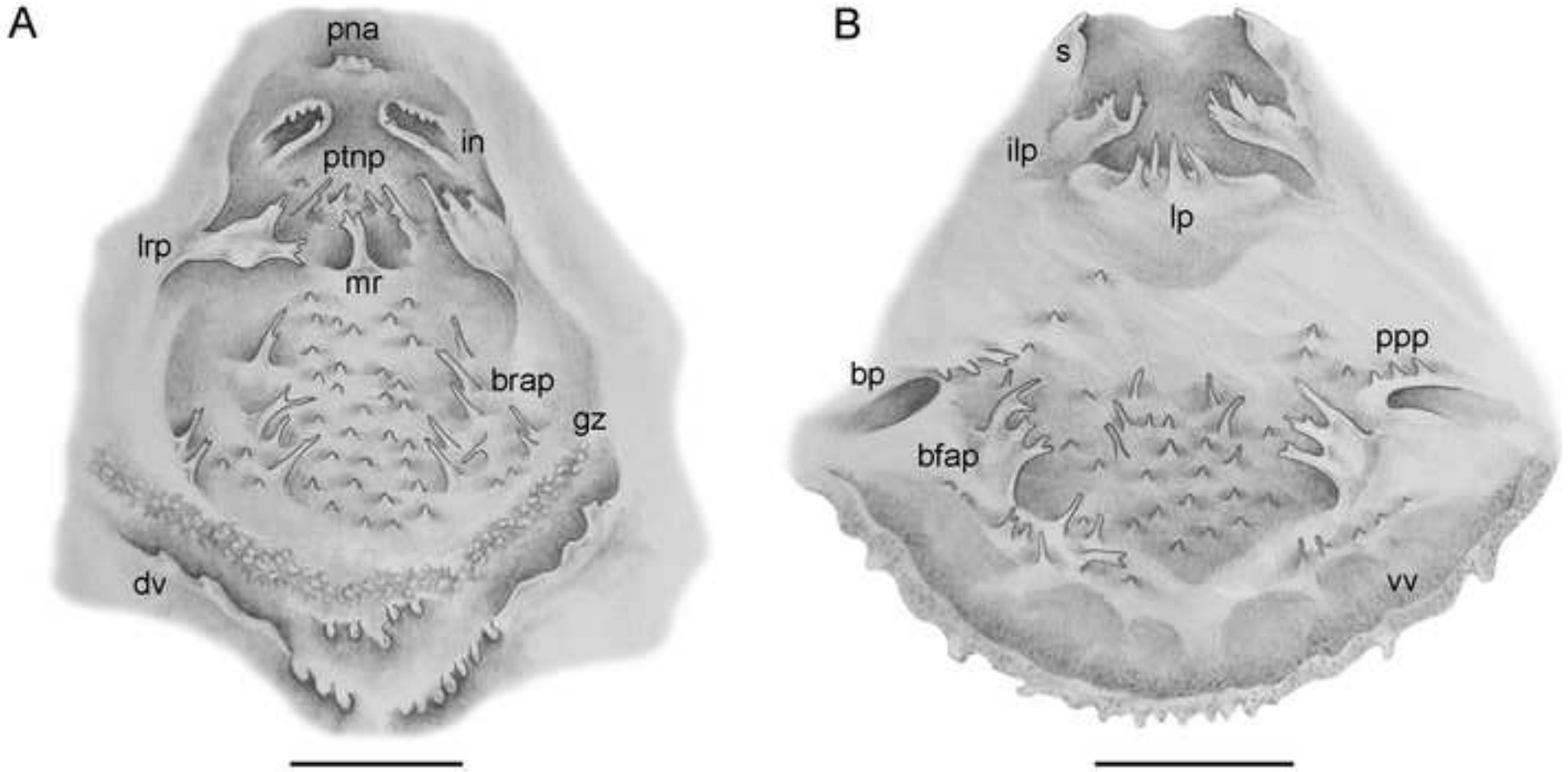

Figure 7

Click here to access/download;Figure;FIG7.tif

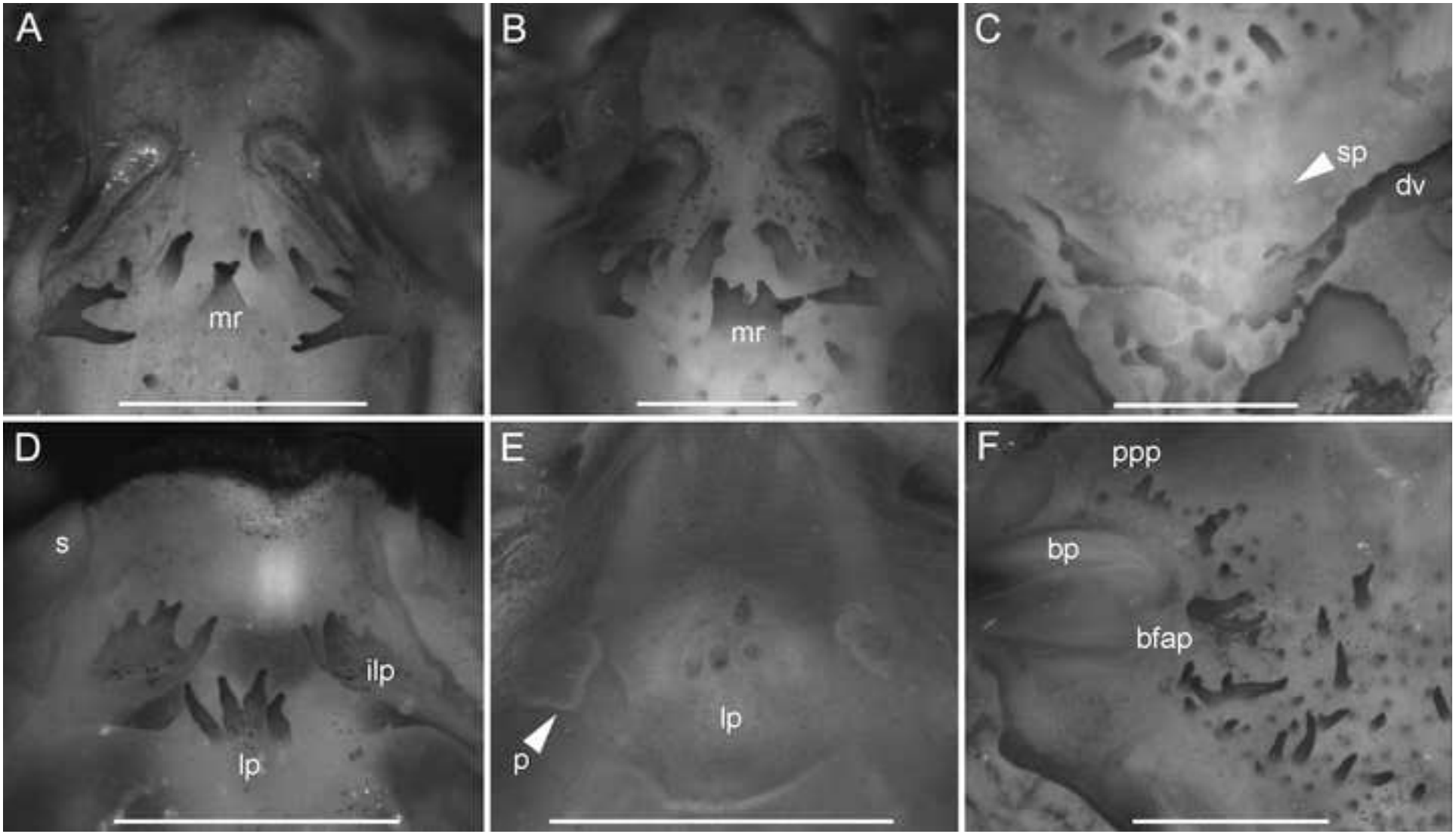

Figure 8

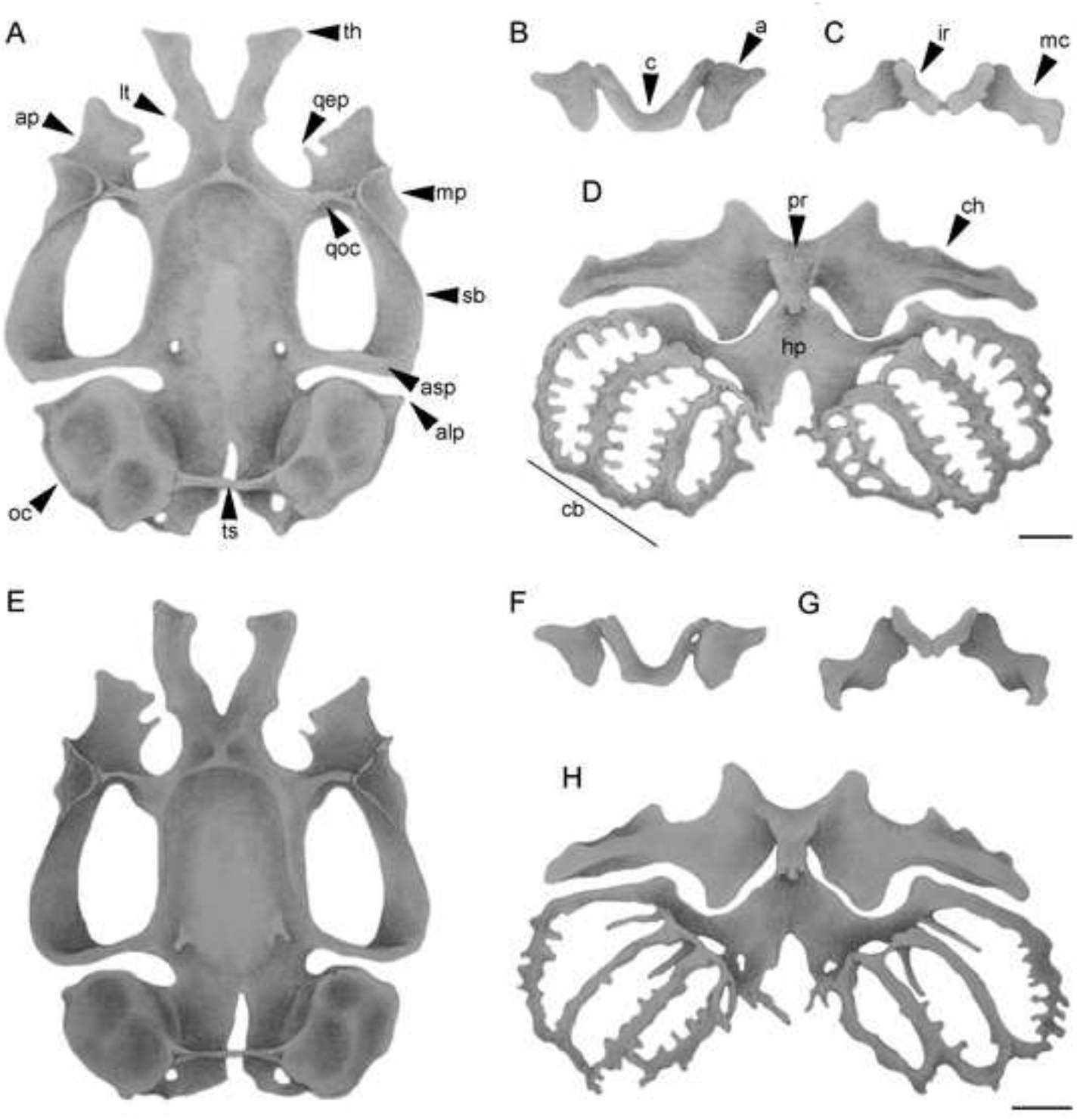

Figure 9

Click here to access/download;Figure;FIG9.tif

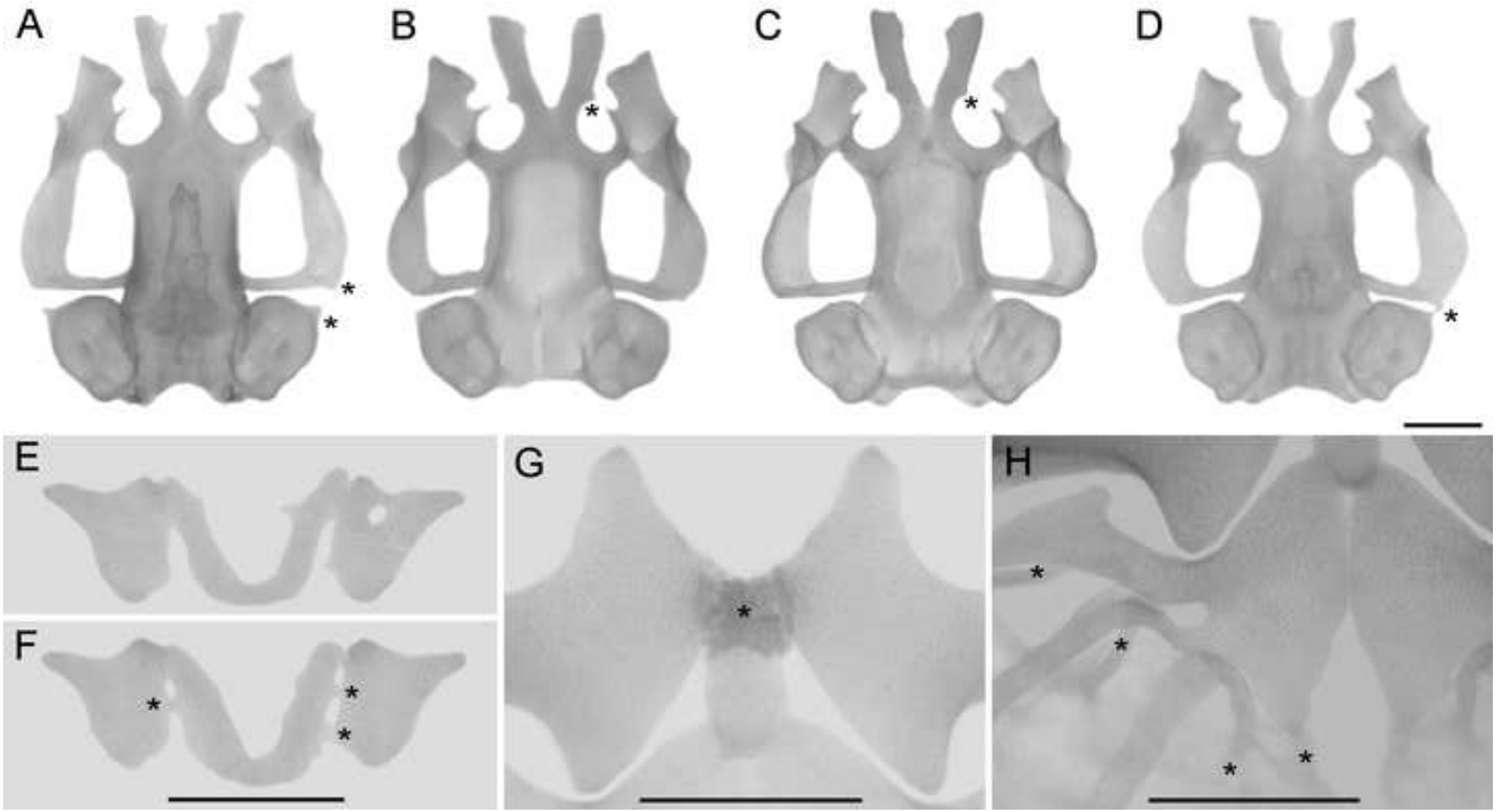

Figure 10